MOLECULAR ECOLOGY

Molecular Ecology (2015) **24**, 83–97 doi: 10.1111/mec.13012

Genetic consequences of postglacial range expansion in two codistributed rodents (genus *Dipodomys*) depend on ecology and genetic locus

TEREZA JEZKOVA,* BRETT R. RIDDLE,* DAREN C. CARD,† DREW R. SCHIELD,† MALLORY E. ECKSTUT* and TODD A. CASTOE†

School of Life Sciences, University of Nevada Las Vegas, 4505 Maryland Parkway, Las Vegas, NV 89154, USA, †Department of Biology, The University of Texas at Arlington, 501 South Nedderman Drive, Arlington, TX 76010, USA

Abstract

How does range expansion affect genetic diversity in species with different ecologies, and do different types of genetic markers lead to different conclusions? We addressed these questions by assessing the genetic consequences of postglacial range expansion using mitochondrial DNA (mtDNA) and nuclear restriction site-associated DNA (RAD) sequencing in two congeneric and codistributed rodents with different ecological characteristics: the desert kangaroo rat (*Dipodomys deserti*), a sand specialist, and the Merriam's kangaroo rat (*Dipodomys merriami*), a substrate generalist. For each species, we compared genetic variation between populations that retained stable distributions throughout glacial periods and those inferred to have expanded since the last glacial maximum. Our results suggest that expanded populations of both species experienced a loss of private mtDNA haplotypes and differentiation among populations, as well as a loss of nuclear single-nucleotide polymorphism (SNP) private alleles and polymorphic loci. However, only *D. deserti* experienced a loss of nucleotide diversity (both mtDNA and nuclear) and nuclear heterozygosity. For all indices of diversity and differentiation that showed reduced values in the expanded areas, *D. deserti* populations experienced a greater degree of loss than did *D. merriami* populations. Additionally, patterns of loss in genetic diversity in expanded populations were substantially less extreme (by two orders of magnitude in some cases) for nuclear SNPs in both species compared to that observed for mitochondrial data. Our results demonstrate that ecological characteristics may play a role in determining genetic variation associated with range expansions, yet mtDNA diversity loss is not necessarily accompanied by a matched magnitude of loss in nuclear diversity.

Keywords: genetic differentiation, genetic diversity, Great Basin, mtDNA sequencing, restriction site-associated DNA sequencing, single-nucleotide polymorphisms

Received 24 March 2014; revision received 16 November 2014; accepted 19 November 2014

Introduction

In a world undergoing rapid climate change, there is great value in being able to predict how the ecological characteristics and evolutionary history of species may influence genetic attributes of populations. The importance of such insight includes the ability to predict when a species may exhibit reduced ability to adapt to global climate change due to reduced genetic variation in parts of its current range. Low population genetic variation can lead to reductions in the fitness of a population, including reduced resistance to competitors, parasites, predators and diseases, in addition to the reduced ability to adapt to environmental change (Lacy 1997; Ouborg 2010; Avolio *et al.* 2012). Genetic diversity typically decreases in response to population decline or fragmentation (Lacy 1997; Joyce & Pullin 2003; Chan *et al.* 2005;

Correspondence: Todd A. Castoe, Fax: 817 272 2855;
E-mail: todd.castoe@uta.edu

Draheim *et al.* 2012) but can also decrease in the context of range expansion events (Hewitt 1996; Excoffier *et al.* 2009). Range expansion can be viewed as a series of founder effects in which a subset of individuals (and a subset of genotypes) from the colonization front disperses into new habitats (Hewitt 1996; Austerlitz *et al.* 1997; Excoffier *et al.* 2009). As a result, more recently established populations may exhibit decreased genetic diversity and heterozygosity within populations, decreased frequencies of private alleles, and decreased genetic differentiation among populations (Hewitt 1996, 2000; Excoffier *et al.* 2009; Kerdelhue *et al.* 2009; Jezkova *et al.* 2011).

Patterns of genetic variation in expanding populations are influenced by the rate and shape of their expansion history (Hewitt 1996; Bialozyt *et al.* 2006; Excoffier *et al.* 2009; Smith *et al.* 2011) and also by the ecological properties of species (Wegmann *et al.* 2006; Excoffier *et al.* 2009; Stone *et al.* 2012). Species-specific influences on such patterns may occur due to ecological properties that determine effective population sizes and patterns of gene flow (Young *et al.* 1996; Joyce & Pullin 2003; Hallatschek & Nelson 2008; Spradling *et al.* 2010). For example, species that have large effective population sizes and high gene flow should tend to retain genetic variation along a colonization front (Joyce & Pullin 2003; Wegmann *et al.* 2006; Excoffier *et al.* 2009). Therefore, more widespread species (e.g. habitat generalists) with high dispersal rates and large population sizes are predicted to exhibit the smallest (if any) decrease in genetic variation following range expansion. Conversely, species with more fragmented distributions (e.g. habitat specialists), lower dispersal rates and lower population sizes should exhibit greater loss of genetic variation oriented in the direction of the expansion event (Joyce & Pullin 2003; Wegmann *et al.* 2006; Smith *et al.* 2011; Stone *et al.* 2012).

Range expansions may occur after speciation events, niche shifts, novel ecological interactions or climate change events (Mila *et al.* 2000; Wegmann *et al.* 2006; Excoffier *et al.* 2009; Kerdelhue *et al.* 2009; Hill *et al.* 2012), such as the rapidly warming climate after the last glacial maximum (LGM; *c.* 21 000 years BP), which triggered major range shifts of many species across the globe (Hewitt 2000). We investigated the genetic consequences of a post-LGM range expansion in two congeneric species that differ in their ecological characteristics but share many other distributional and life history attributes. The desert kangaroo rat (*Dipodomys deserti*) is a sand substrate specialist that has a more fragmented distribution and smaller population sizes than Merriam's kangaroo rat (*Dipodomys merriami*), a substrate generalist that can live equally well in sandy soils, clays, gravels and rocks (Brown 1973; Best *et al.* 1989). Currently, these two species occur sympatrically throughout the warm Mojave and Sonoran deserts and along a low-elevation corridor within the cold Great Basin Desert (Fig. 1A,B). Palaeontological and palaeoenvironmental evidence suggests, however, that neither species was present in the northern Mojave Desert and the Great Basin until the Late Pleistocene or perhaps until the beginning of the Holocene (Spaulding 1990b; Thompson 1990; Hockett 2000). Both species likely persisted within the warmer southern Mojave and Sonoran deserts during the cold glacial period, and together with other warm desert taxa, expanded northwards after the LGM (Mulcahy 2008; Jezkova 2010; Graham *et al.* 2013).

Here, we tested the hypothesis that the different ecological properties exhibited by these two species have led to different population genetic effects of range expansion from the southern warm deserts (Sonoran and southern Mojave deserts) into the northern cold deserts (northern Mojave and Great Basin deserts). Specifically, we tested the prediction that the sand specialist, *D. deserti*, experienced a greater loss of genetic diversity and differentiation in the direction of the expansion than the habitat generalist, *D. merriami*. To test this, we constructed climatic niche models projected onto simulated LGM conditions to approximate the distribution of each species during this time period. We then assessed, for both species, whether genetic variation differs between populations that have persisted throughout glacial periods (referred to as 'stable'), and those that likely expanded northwards only after the LGM (referred to as 'expanded'). We then asked whether mitochondrial DNA (mtDNA) and nuclear single-nucleotide polymorphism (SNP) data provide congruent estimates of patterns of genetic variation between expanded and stable populations as well as between species.

Materials and methods

Taxon sampling

We acquired samples from 328 individual *Dipodomys deserti* from 56 localities spanning the entire range of this species (the Sonoran, Mojave and Great Basin deserts) (Fig. 1A; Data S1, Supporting information). *Dipodomys merriami* has a larger distribution than *D. deserti* as it also occurs in the Chihuahuan and Baja California deserts (Alexander & Riddle 2005). For the purpose of this study, we included *D. merriami* populations distributed throughout the three target desert regions that overlap with *D. deserti*. We acquired 210 samples of *D. merriami* from 49 localities (Fig. 1B; Data S1, Supporting information). Samples of *D. deserti* from Mexico ($N = 24$) were acquired from the Museum of Vertebrate Zoology, University of California. All other animals were specifically captured for this study ($N = 486$) and either ear-clipped and released or euthanized following

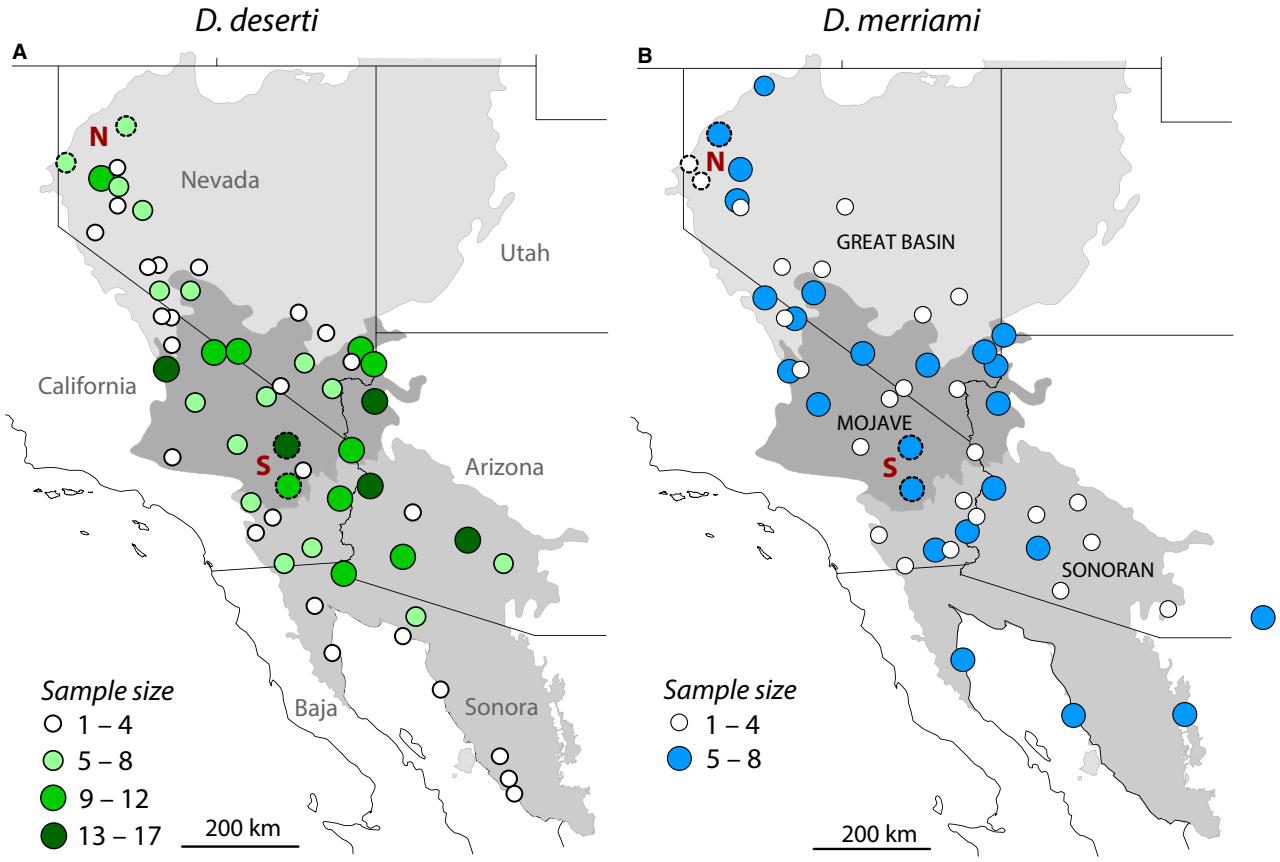

Fig. 1 Sampling locations and sample sizes for *Dipodomys deserti* (A) and *Dipodomys merriami* (B) for mtDNA (all circles) and ddRAD [dashed circles, labelled North (N) and South (S)]. Grey-shaded areas represent the three target desert regions: Sonoran, Mojave and the Great Basin deserts.

methods approved by the American Society of Mammalogists (Sikes *et al.* 2011) and the Animal Care and Use Committee at the University of Nevada Las Vegas, with vouchers deposited at the New Mexico Museum of Natural History (Data S1, Supporting information). All samples were used for mtDNA sequencing and analysis. For double-digest restriction site-associated DNA sequencing (ddRADseq) sampling, we selected two general areas, one within the southern Mojave Desert (representing temporally stable populations) and one within the northern Great Basin (representing expanded populations; Fig. 1A,B). For each area and each species, we sampled 8–10 individuals (for a total of 19 *D. deserti* from two southern and two northern sites and 18 *D. merriami* from two southern and three northern sites; Fig. 1A,B; Data S1, Supporting information).

Ecological niche models

We modelled the climatic niche of *D. deserti* and *D. merriami* to approximate the current and LGM distribution of each species. We applied ecological niche modelling methods, where environmental data are extracted from current occurrence records, and habitat suitability is evaluated across the landscape using programme-specific algorithms (Elith *et al.* 2006). The present-day models were then projected on the climatic reconstructions of the LGM under the assumption that the climatic niche of each species remained conserved between the LGM and present (Elith *et al.* 2010).

For occurrence data, we used museum records downloaded from the Manis Database (http://manisnet.org/) from which we excluded records that had a coordinate uncertainty larger than 5 km. To reduce spatial bias caused by unequal sampling (Boria *et al.* 2014; Radosavljevic & Anderson 2014), we plotted all records on a map over a grid of 25 × 25 km and retained only one random record in each grid cell. Our final data sets comprised 143 records for *D. deserti* and 220 records for *D. merriami*. The current climate was represented by bioclimatic variables from the WorldClim dataset v. 1.4 (Hijmans *et al.* 2005). We followed the methodology of Jezkova *et al.* (2011) to remove highly correlated variables (i.e. with a correlation coefficient > 0.9), resulting in selection of 14 predictor variables. For environmental layers representing the climatic conditions of the LGM,

we used two models of ocean–atmosphere simulations available through the Paleoclimatic Modelling Intercomparison Project (Braconnot *et al.* 2007): the Community Climate System Model v. 3 (CCSM) and the Model for Interdisciplinary Research on Climate v. 3.2 (MIROC).

Climatic niche models were constructed in MAXENT v. 3.3.3k (Phillips *et al.* 2006), which estimates relative probabilities of the presence of species within defined geographic spaces, with high probabilities indicating suitable environmental conditions for the species (Phillips *et al.* 2004). Our models were confined to the southwest region of North America. We used the default parameters in MAXENT (500 maximum iterations, convergence threshold of 0.00001, regularization multiplier of 1 and 10 000 background points) with the application of random seed and logistic probabilities for the output (Phillips & Dudik 2008). We ran 50 replicates for each model, and an average model was presented using logistic probability classes of climatic niche suitability. The presence–absence map was determined using a threshold that balances omission, predicted area and a threshold value (Liu *et al.* 2005). We used the receiver operating characteristic to determine an area under the curve (AUC) value to evaluate model performance, where AUC values range from 0.5 for a random prediction to 1 for perfect prediction (Raes & ter Steege 2007).

Laboratory methods—mtDNA sequencing

We isolated total genomic DNA from fresh-preserved heart, kidney, liver or ear tissue following the protocol for the DNeasy Extraction Kit (Qiagen Inc.). We amplified an ~1000 base-pair (bp) fragment of the mitochondrial control region using the primers L15926DIOR (5′-GTATAAAAATTACTCAGGTCTTGT-3′) and H651 (Kocher *et al.* 1989). Amplifications were conducted using Takara Ex Taq Polymerase Premix (Takara Mirus Bio, Inc.), and a thermocycling profile including 40 amplification cycles, and a 55 °C annealing temperature. Amplifications were cleaned before sequencing using ExoSap-IT (USB Corp.). Amplified products were sequenced in both directions using *Dipodomys*-specific primers, L16007DiDe (5′-CCCAAAGCTGGAATTTTAA-3′) and H16498DiDe (5′-CCTGAGGTAAGAACCA-GATG-3′), and the BIGDYE TERMINATOR v3.1 Cycle Sequencing Kit run on an ABI Prism 3130 (Applied Biosystems, Inc.). DNA from museum skins was isolated as described above with the following modifications: 40 μL proteinase K (double the regular value), 30 μL DDT added prior to incubation and a 3-day digestion period. These extractions were conducted in a separate laboratory where *Dipodomys* have never previously been processed. For these lower quality DNA samples, the mitochondrial control region was amplified using five overlapping amplification products of about 250 bp each using GoldTaq (Life Technologies).

Laboratory methods—RAD sequencing

We estimated nuclear genetic variation using genome-wide sampling of SNPs from thousands of loci using ddRAD sequencing (Jones *et al.* 2012; Peterson *et al.* 2012). We generated ddRAD libraries for 19 *D. deserti* and 18 *D. merriami* individuals following the protocol of Peterson *et al.* (2012). Genomic DNA was simultaneously cut with *Sbf*I and *Sau*3AI restriction enzymes. Double-stranded indexed DNA adapters that contained unique molecular identifiers (UMIs; eight consecutive *N*'s prior to the ligation site) were ligated to the ends of digested fragments. Following adapter ligation, samples were pooled in sets of 8, and these pools were size selected for a range of 390–440 bp using a Blue Pippin device (Sage Science). After size selection, samples were PCR amplified with pool-specific indexed primers, and amplification products were further pooled into a single sample based on molarity calculations from analysis on a Bioanalyzer (Agilent) using a DNA 7500 chip. The final pooled library was sequenced using 100-bp paired-end reads on an Illumina HiSeq 2000 lane.

MtDNA analyses

Chromatograph files of mtDNA control region sequences were edited, combined and aligned using SEQUENCHER v. 5.1 (Gene Codes Corp.), and basic sequence statistics were calculated in MEGA v. 5.1 (Tamura *et al.* 2011). We constructed median-joining networks (Bandelt *et al.* 1999) to reconstruct relationships among haplotypes in the program NETWORK v. 4.5.1.6 (Bandelt *et al.* 1999).

We analysed changes in effective population size through time for each species using the Bayesian skyline coalescent method (Drummond *et al.* 2005) implemented in BEAST v. 1.8.0 (Drummond & Rambaut 2007). For these analyses, we used the HKY substitution model, a strict molecular clock and a coalescent Bayesian skyline as a tree prior to five skyline groups for all runs. We applied two mutation rates that represent a range of mutations previously used for the mtDNA control region in small mammals: 1.5% and 6% × lineage^{-1} million × years^{-1} (Martin & Palumbi 1993; Galbreath *et al.* 2009; Jezkova *et al.* 2011), although we note that the mtDNA mutation rate in heteromyids is most likely closer to the faster rate (Spradling *et al.* 2001). For each mutation rate, we conducted two independent Markov chain Monte Carlo runs of 200 million generations, and discarded the first 25% of generations as burn-in. Posterior samples from the two runs were

combined in LogCombiner (Drummond & Rambaut 2007), and Tracer v. 1.5 was used to confirm convergence of all parameters (ESS values > 200) and to reconstruct the Bayesian skyline plots (BSP).

We compared mtDNA patterns across the species ranges using three genetic measures: genetic diversity within populations, frequency of private haplotypes within populations and genetic differentiation among populations. Genetic diversity within populations was represented by nucleotide diversity calculated in arlequin v. 3.11 (Excoffier *et al.* 2005), and frequencies of private haplotypes within populations (i.e. frequencies of haplotypes endemic to a population) were manually calculated. Both indices were only calculated for sampling localities with five or more samples (31 and 25 localities for *D. deserti* and *D. merriami*, respectively; Fig. 1A,B). Values for both indices were imported into arcgis v. 9.2 (ESRI) and interpolated across uniformly spaced 2.5-minute grids to visualize mtDNA patterns across the landscape. We used the inverse distance weighted interpolation procedure (Watson & Philip 1985) in the Spatial Analyst extension of arcgis and masked the interpolations to our ecological niche models for current climatic conditions. To confirm that population sample sizes were sufficient for calculating nucleotide diversity and frequencies of private haplotypes, we calculated the Pearson's product-moment correlation coefficient between these indices and sample size in r v. 3.0.0 (R Development Core Team 2008).

Genetic differentiation among populations was represented by average pairwise genetic distances between sequences from neighbouring sampling sites calculated in alleles in space v. 1.0 (Miller 2005). Residual genetic distances, derived from the linear regression of genetic vs. geographical distance, were assigned to mid-points between sampling sites using the Delaunay triangulation-based connectivity network, imported into arcgis and interpolated across the landscape, as described above. Lastly, we calculated Pearson's product-moment correlation coefficient in *R* to statistically assess the relationships between latitude and the three mtDNA indices: nucleotide diversity, frequency of private haplotypes and pairwise genetic distances.

Nuclear SNP—RADseq analyses

Raw Illumina sequence data were filtered to remove PCR clones (totalling 1% of raw reads) identified by UMIs integrated into our adapters using the *clone_filter* program in the stacks pipeline (Catchen *et al.* 2011). Low-quality reads and reads lacking the restriction cut-site sequences were also discarded using the *process_radtags* program from stacks. The genome of *Dipodomys ordii* (assembly dipOrd1 release 73) was used as a reference for mapping ddRADseq reads in CLC Genomics Workbench (CLC Bio/Qiagen), using a mismatch cost of 2, insertion cost of 3, deletion cost of 3, length fraction of 0.5 and similarity fraction of 0.8. Mapping output was then run through the stacks pipeline. To verify consistency in population genetic estimates under various parameter settings, we applied two thresholds for the minimum number of reads per stack (10 and 20), and filtered the data based on two thresholds of allowance for missing data across individuals at a locus (50% and 75%) using the *populations* program in stacks. For each species, we used stacks to calculate the mean for the number of all loci and the percentage of polymorphic loci, nucleotide diversity (Pi), heterozygosity, frequency of private alleles, and to estimate F_{ST} between stable and expanded populations. Standard error for the nucleotide diversity, heterozygosity and F_{ST} was also calculated in stacks while the standard error for private alleles was assessed from 1000 bootstrap replicates using a custom python script.

Results

Ecological niche models

The ecological niche models based on present-day climate conditions (Fig. 2A,B) captured the known distribution of both species well, as suggested by AUC values of 0.881 and 0.858 for *Dipodomys deserti* and *Dipodomys merriami*, respectively. The presence–absence threshold corresponded to logistic probabilities of 0.07 for *D. deserti* and 0.08 for *D. merriami*. The LGM models (Fig. 2C,D) indicate unsuitable climatic niches in the northern and eastern Mojave Desert, Great Basin Desert and eastern Sonoran Desert for both species. Suitable climatic niches during the LGM are inferred to have existed within the southern Mojave, western Sonoran Desert and adjacent Baja California Desert, including some areas in the Gulf of California currently under water (Fig. 2C,D). A suitable niche was also inferred for *D. merriami* in southeastern Sonoran Desert, but this area also exhibits high clamping values (i.e. extrapolation beyond training values) and therefore should be interpreted with caution.

MtDNA analyses

We obtained 1000 and 960 bp of the mtDNA control region for *D. deserti* and *D. merriami*, respectively. We identified 149 unique haplotypes for *D. deserti* and 161 for *D. merriami* (Fig. 3A,B). The intraspecific mean divergence was similar in both species: 0.018 (±0.002)

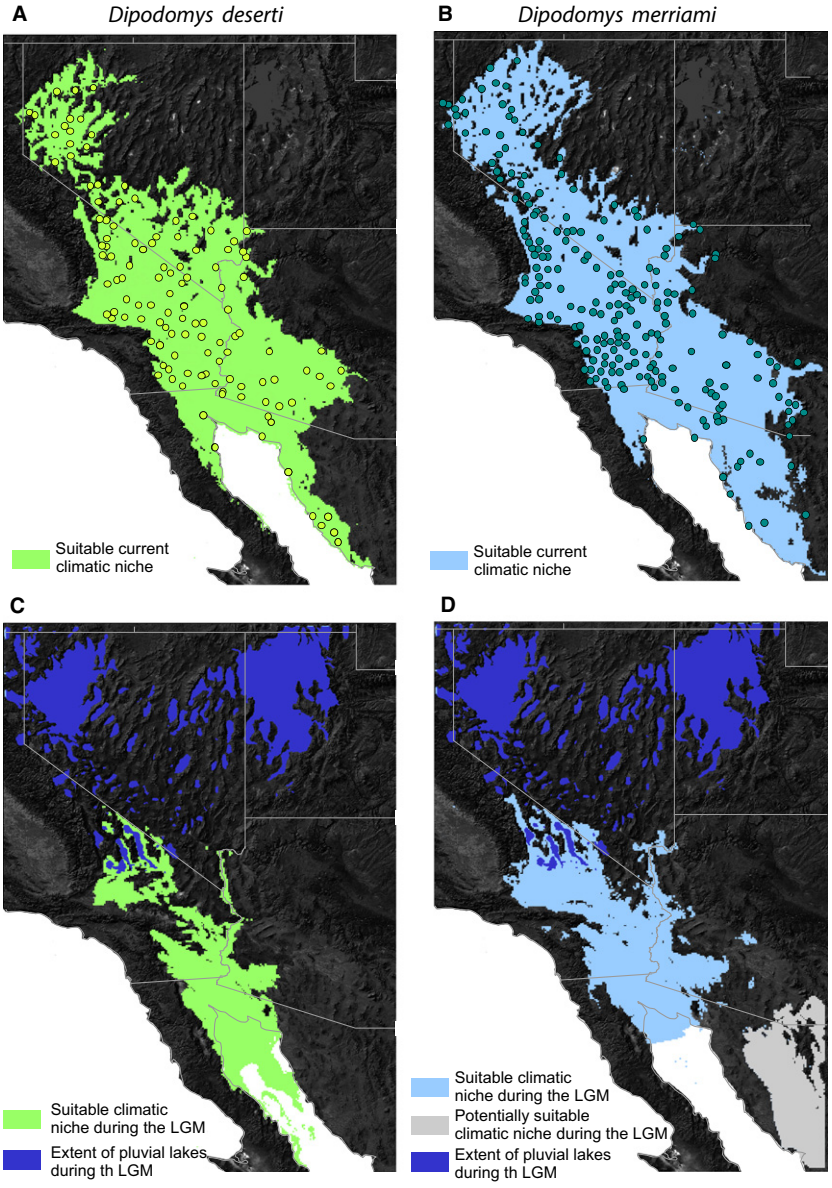

Fig. 2 Climatic niche models for *Dipodomys deserti* and *Dipodomys merriami* based on 14 bioclimatic variables. Green (A, C) and blue (B, D) shading represents suitable climatic conditions for present (A, B) and the last glacial maximum (LGM) (C, D), using a threshold for logistic probabilities that balances omission, predicted area and a threshold value. Dots in A and B represent occurrence records used to build models. The dark blue shading in C and D shows the extent of pluvial lakes during the LGM. The grey shading in D was inferred as suitable for *D. merriami* but also exhibits high clamping values (see text for details).

for *D. deserti* and 0.019 (±0.002) for *D. merriami*. Despite similar intraspecific levels of divergence, the haplotype networks of the two species illustrate quite different phylogenetic and phylogeographic patterns. In *D. deserti*, haplotypes are better sorted within populations (Fig. 3A), while *D. merriami* exhibits a star-shaped network for the majority of the sampling region (Fig. 3B). The BSPs indicate larger effective population sizes through time in *D. merriami* than in *D. deserti* (Fig. 3A, B, insets). The plot for *D. deserti* (Fig. 3A, inset) shows constant population size followed by a rapid population expansion dated to *c.* 25 000 and 100 000 years BP using the faster and slower mutation rates, respectively. The plot for *D. merriami* shows a more gradual increase in population size with a rapid demographic expansion dated to *c.* 25–50 000 years BP (using the faster mutation rate) and 100–200 000 years BP (using the slower mutation rate) (Fig. 3B, inset).

The genetic landscape maps revealed low nucleotide diversities in *D. deserti* within the northern and eastern Mojave Desert, as well as the Great Basin Desert (Fig. 4A). Remaining portions of the sampled range of this species exhibited moderate-to-high nucleotide diversity (Fig. 4A). Areas with the lowest frequencies of private haplotypes and pairwise distances for *D. deserti* correspond well with those areas that show low nucleotide diversity (Fig. 4B,C). In contrast, landscape genetic maps of *D. merriami* demonstrate mitochondrial nucleotide diversities that are moderate to high across all three desert regions (Fig. 4A). The private haplotype

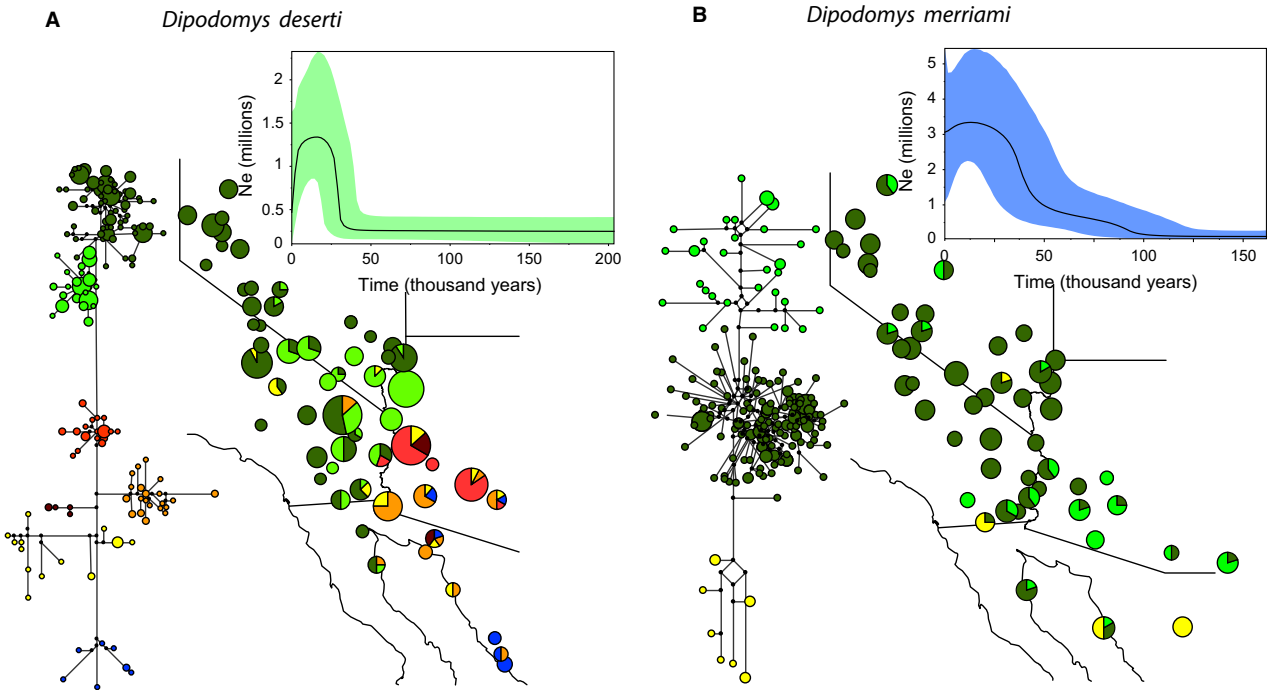

Fig. 3 Median-joining network of mtDNA haplotypes for 328 samples of *Dipodomys deserti* (A) and 210 samples of *Dipodomys merriami* (B). Circle size reflects the number of individuals exhibiting that haplotype. The length of connection lines between haplotypes is proportional to the number of mutational changes. The main haplogroups are colour-coded and plotted on the map. Insets: Bayesian skyline plots (BSP) showing the change in effective population size (*y*-axis) over time (*x*-axis). Black solid lines indicate the median value of effective population size, and green and blue shading denotes the 95% highest posterior probability interval. The time on *x*-axis is based on a mutation rate of 6% lineage^{-1} million years^{-1}.

frequencies are generally higher in *D. merriami* than in *D. deserti* with a clear trend of higher values within the stable areas and lower values in the expanded areas (Fig. 4B). Pairwise genetic distances for *D. merriami* show similar levels of differentiation across the range as those for *D. deserti*, and are highest within the southern deserts and lower in the northern range extents (Fig. 4C).

In *D. deserti*, but not in *D. merriami*, there was a significant negative correlation between nucleotide diversity and latitude (Fig. 4A, insets). Frequencies of private haplotypes and pairwise genetic distances had significant negative correlations with latitude for both species (Fig. 4B,C, insets). Nucleotide diversity was not significantly correlated with sample size for either species, while the frequency of private haplotypes was significantly correlated with sample size in *D. deserti*, but not in *D. merriami* (Fig. S2, Supporting information). The significant correlation between private allele frequency and latitude persisted, however, even when a rarefaction analysis (resampling 20 times for a fixed value of five samples per site) was conducted (*D. deserti*: $r = -0.684$, $P < 0.0001$; *D. merriami*: $r = -0.673$, $P < 0.0001$).

Nuclear SNP variation

Statistics based on the number of reads retained after processing steps in the ddRAD pipeline for each sample are provided in Table S1 (Supporting information), while population genetic statistics, including the number of polymorphic loci, nucleotide diversity (average number of pairwise nucleotide differences per site in a population), heterozygosity, frequency of private alleles (i.e. number of private alleles/number of variable SNPs) and F_{ST} values, are shown in Figs 5 and 6 and Table 1. These estimates are provided for multiple filtering thresholds of the SNP data, although all qualitative patterns and trends between species and populations were consistent across thresholds (Table 1). The 10× coverage and 50% minimum individuals per locus per population threshold yielded 13 276 variable SNPs (representing 12 769 loci) within *D. deserti* and 15 798 variable SNPs (representing 13 954 loci) within *D. merriami*.

We found similar proportions of polymorphic loci in *D. deserti* and *D. merriami* and a decrease in polymorphic loci in northern (expanded) vs. southern (stable) populations in both species, with a greater

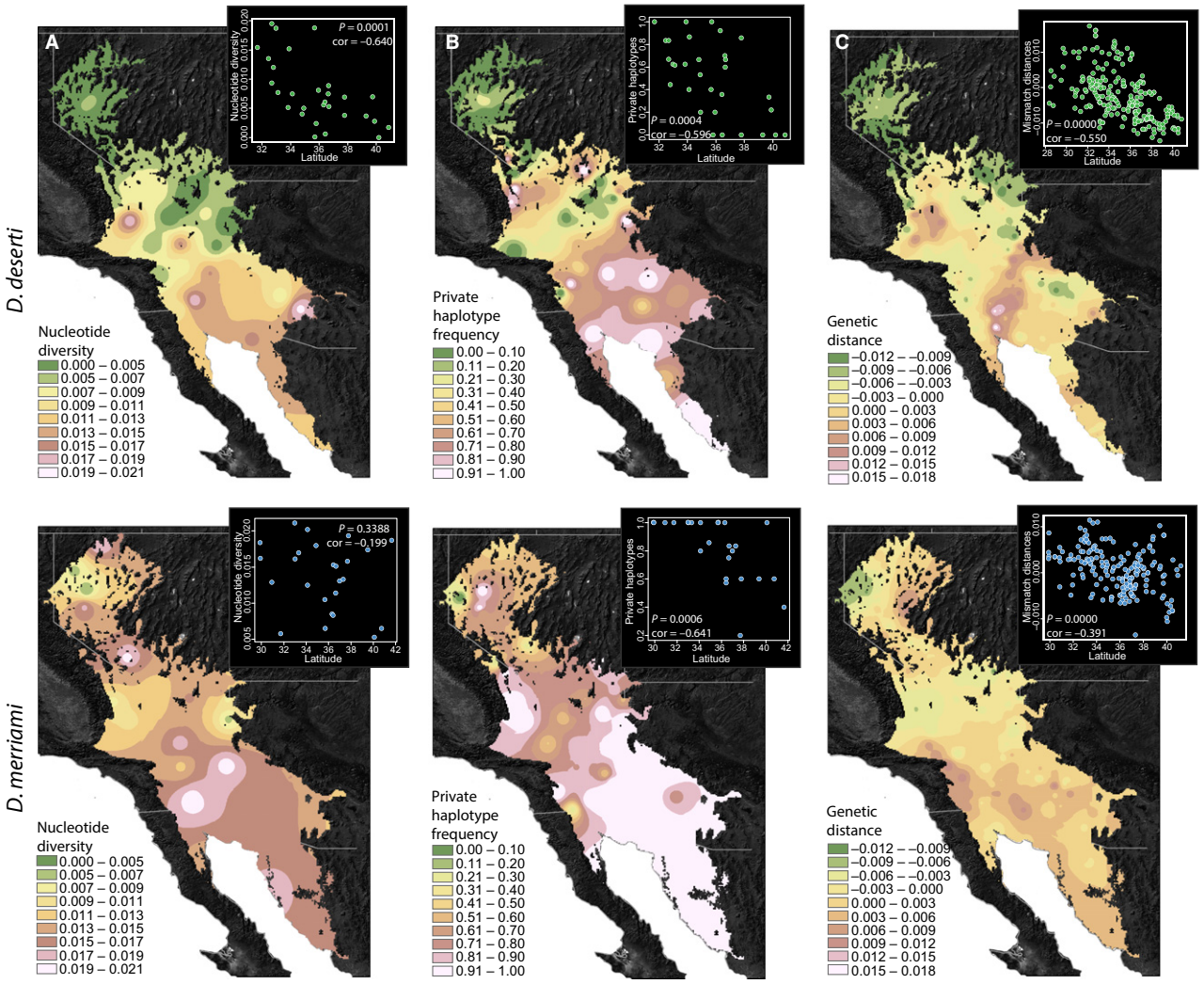

Fig. 4 Nucleotide diversity (A), frequency of private haplotypes (B) and pairwise genetic distances (C) calculated from mtDNA sequences and interpolated across landscape for *Dipodomys deserti* (top) and *Dipodomys merriami* (bottom). The interpolations were restricted to the current climatic niche model of each species. Insets: correlations between each genetic index and latitude. Correlation coefficient and associate *P*-values are indicated for each comparison.

decrease in *D. deserti* (Fig. 5A; Table 1). Estimates of nucleotide diversity and heterozygosity were similar in the stable populations of both species, and while *D. deserti* exhibited decreases in nucleotide diversity and heterozygosity in expanded populations, *D. merriami* exhibited similar values in both areas (Fig. 5B,C; Table 1). Private allele frequencies were similar in stable populations of both species. Both species exhibit loss of private allele frequencies in expanded populations, with *D. deserti* experiencing a more pronounced loss of private alleles than *D. merriami* (Fig. 5D; Table 1). Finally, nuclear SNP F_{ST} values show greater differentiation between the stable and expanded populations of *D. deserti* than those of *D. merriami* (Fig. 6; Table 1).

Discussion

Assessing the impacts of population history and ecology on genetic patterns

We conducted a comparative assessment of the genetic consequences of a post-LGM range expansion in two sympatric rodents with differences in habitat specialization using both mtDNA and ddRADseq (i.e. nuclear) markers. Our analyses revealed links between genetic patterns, population history and species-specific ecological characteristics. In both species, we observed differential population genetic characteristics between populations inferred to have persisted during the latest glacial period and those that expanded only

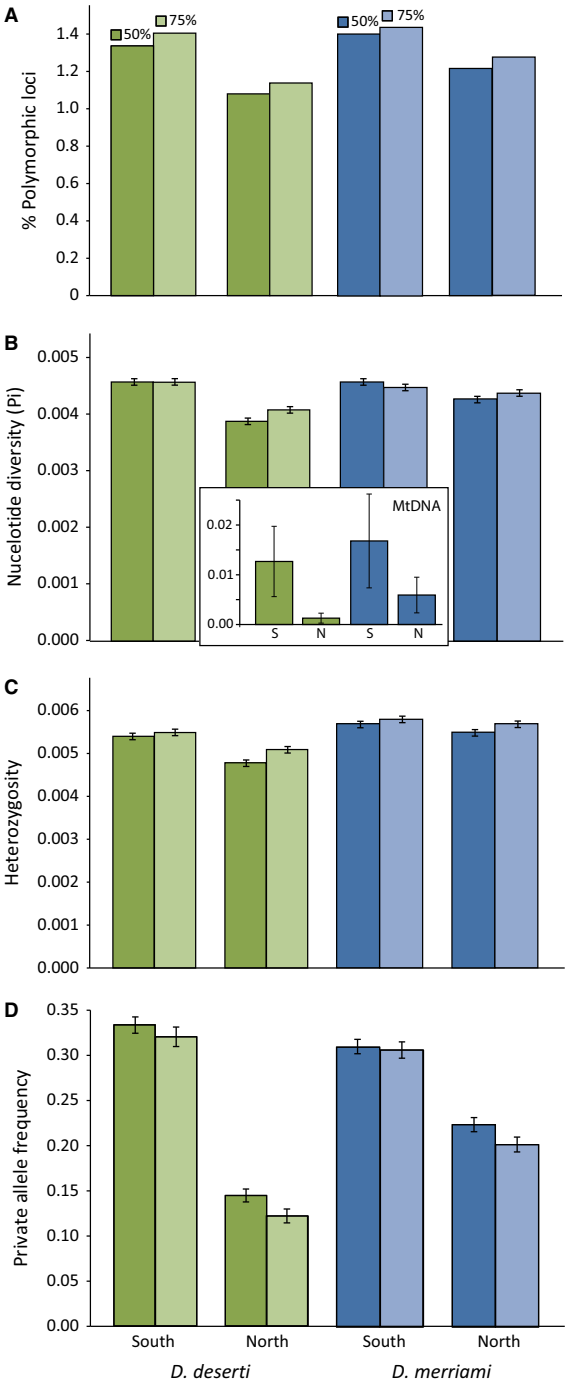

Fig. 5 Numbers of polymorphic loci (A), nucleotide diversity (B), heterozygosity (C) and frequencies of private alleles (D) for northern and southern populations of *Dipodomys deserti* and *Dipodomys merriami* based on single-nucleotide polymorphisms (SNPs) recovered from two data filtering thresholds in the 'populations' program in STACKS. The thresholds were set such that only loci present in 50% or 75% of individuals in each population (i.e. north vs. south) at 10× coverage were used to estimate parameters. The inset in B shows mtDNA patterns of nucleotide diversity for the same 37 samples used in the SNP assessment.

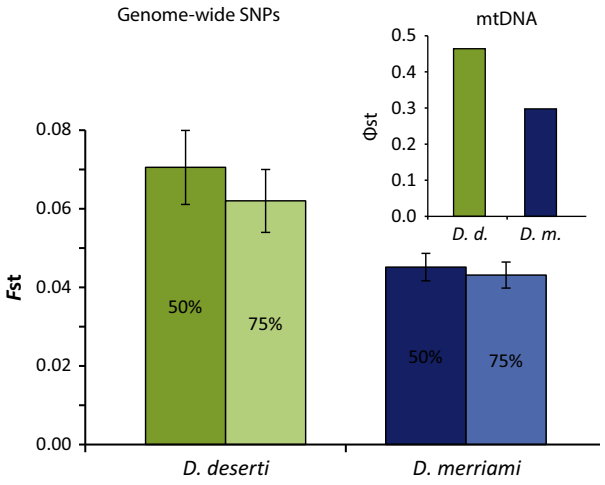

Fig. 6 Estimates of F_{ST} for *Dipodomys deserti* and *Dipodomys merriami* based on single-nucleotide polymorphisms (SNPs) recovered from two filtering thresholds in the 'populations' program in STACKS. The filters were set such that only loci present in 50% or 75% of individuals in each population (i.e. north vs. south) at 10× coverage were used. Inset: estimates of Φ_{ST} from mtDNA sequences for the same 37 samples used in the SNP assessment.

after the LGM. The substrate specialist *Dipodomys deserti*, however, exhibited more pronounced changes in genetic structure associated with the range expansion than the substrate generalist, *Dipodomys merriami*. Additionally, we identified remarkably large quantitative differences in mitochondrial vs. nuclear patterns of genetic diversity and differentiation associated with range expansion, likely reflecting that these markers differ in their nature of inheritance, effective population size and/or sex-biased patterns of gene flow. Our results suggest that mtDNA may be more sensitive for the detection of historical range expansion compared to nuclear loci, yet patterns of mtDNA may provide misleadingly low estimates of nuclear genetic diversity and thus future adaptive potential of populations. Collectively, our results provide evidence for the synergistic interaction of ecology and population history on population genetic variation that might in turn impact the ability of populations to evolve in response to environmental change.

Genetic and palaeoenvironmental evidence of population expansions since the LGM

Our genetic analyses and estimates from past climate-based niche modelling broadly agree and indicate that the ranges of both species have expanded northwards since the LGM. Our climate niche models indicate that the northern and eastern Mojave Desert and the Great Basin Desert were climatically unsuitable for both

Table 1 Genome-wide population parameters calculated from single-nucleotide polymorphisms (SNPs) from ddRAD sequencing for *Dipodomys deserti* and *Dipodomys merriami*. The mean number of polymorphic loci and per cent of polymorphic loci (polymorphic loci/all loci), mean and variance of the number of individuals (Indv), mean and standard error (StdErr) of nucleotide diversity (Pi), heterozygosity, frequency of private alleles and F_{ST} values are shown. Coverage refers to the minimum number of reads per stack per individual (10×, 20×), and threshold (Thres) represents different allowances for missing data (50% and 75%)

		Indv		Polymorphic		% Polymorphic		Pi		Heterozygosity		Private alleles		
	Thres (%)	South	North	South	North	South	North	South	North	South	North	South	North	F_{ST}
Dipodomys deserti														
Coverage: 10×														
Mean	50	8.2	7.5	11 753	10 070	1.33	1.08	0.0046	0.0039	0.0054	0.0048	0.32	0.14	0.0705
	75	9.4	8.3	8056	7673	1.40	1.14	0.0046	0.0041	0.0055	0.0051	0.31	0.12	0.0620
Variance/StdErr	50	3.4	2.2					4.6E-5	4.3E-5	6.1E-5	5.9E-5	0.0087	0.0069	0.0094
	75	0.7	0.7					5.6E-5	5.1E-5	7.6E-5	7.1E-5	0.0104	0.0074	0.0080
Coverage: 20×														
Mean	50	7.7	7.0	6715	6273	1.33	1.06	0.0047	0.0039	0.0057	0.0049	0.29	0.14	0.0678
	75	9.0	7.9	4089	4354	1.45	1.18	0.0049	0.0043	0.0063	0.0055	0.29	0.10	0.0589
Variance/StdErr	50	3.0	1.8					6.2E-5	5.3E-5	8.4E-5	7.6E-5	0.0109	0.0084	0.0090
	75	0.7	0.6					8.4E-5	7.0E-5	1.2E-4	1.0E-4	0.0142	0.0087	0.0075
Dipodomys merriami														
Coverage: 10×														
Mean	50	7.7	7.9	14 431	12 498	1.39	1.22	0.0046	0.0043	0.0057	0.0055	0.31	0.22	0.0451
	75	8.3	8.5	11 412	10 444	1.44	1.27	0.0045	0.0044	0.0058	0.0057	0.31	0.20	0.0431
Variance/StdErr	50	2.0	1.9					4.2E-5	4.3E-5	6.0E-5	6.1E-5	0.0076	0.0076	0.0035
	75	0.6	0.6					4.8E-5	4.8E-5	6.9E-5	6.9E-5	0.0087	0.0079	0.0033
Coverage: 20×														
Mean	50	7.2	7.7	8026	7163	1.32	1.20	0.0044	0.0044	0.0058	0.0059	0.28	0.20	0.0466
	75	8.0	8.3	5723	5709	1.34	1.24	0.0044	0.0045	0.0060	0.0062	0.28	0.18	0.0421
Variance/StdErr	50	1.8	1.9					5.5E-5	5.7E-5	8.0E-5	8.4E-5	0.0100	0.0094	0.0039
	75	0.6	0.6					6.6E-5	6.5E-5	9.8E-5	9.9E-5	0.0119	0.0100	0.0034

species during the LGM (Fig. 2A,B). Similarly, LGM environmental reconstructions (Spaulding 1983, 1990a; Thompson 1990) indicate that the low-elevation habitats within the northern Mojave and Great Basin deserts were covered with large pluvial lakes during the LGM (Grayson 1993; Reheis 1999) or replaced by an assemblage of plants currently found in higher elevations (Spaulding 1983, 1990a; Thompson 1990; Grayson 1993). Accordingly, lower elevation desert habitats were not established until the end of the Pleistocene or even the beginning of the Holocene, when the climate warmed, plant communities shifted upslope and northwards and the large pluvial lakes desiccated (Spaulding 1990a; Thompson 1990). This new habitat allowed many warm-adapted species to expand northwards (Jones 1995; Britten & Rust 1996; Mulcahy 2008; Graham *et al.* 2013). The establishment of sand dunes, the prime habitat for *D. deserti*, is directly tied to sand deposition within pluvial lake basins, followed by aeolian transport after the LGM (Smith 1993). The palaeontological record also supports post-LGM range expansion of these taxa northwards, as the earliest fossils of *D. deserti* or *D. merriami* from the northern Mojave Desert are dated to *c.* 12 000 years BP (Hockett 2000), and those from the Great Basin Desert to *c.* 8100 years BP (Neotoma Paleoecology Database; http://www.neotomadb.org/).

Our genetic results generally support post-LGM expansion of *D. deserti* and *D. merriami* northwards. Allelic diversity and heterozygosity are predicted to be higher in stable populations (i.e. refugia; Grassi *et al.* 2009; Jezkova *et al.* 2011; Maggs *et al.* 2008) and to decrease in the direction of the expansion due to compounding founder effects. Similarly, higher frequencies of private alleles are often used to infer population persistence (Hewitt 1996; Austerlitz *et al.* 1997; Excoffier *et al.* 2009; White *et al.* 2013). Our mtDNA and nuclear DNA estimates of genetic diversity and differentiation are generally consistent with these predictions, except we did not find lower levels of nucleotide diversity (both mtDNA and nuclear) and heterozygosity in the expanded areas of *D. merriami* (Figs 4A and 5B,C). We believe that this pattern is tied to the generalist ecology of *D. merriami* and discuss this further below. Our BSP assessment of demographic change through time is broadly consistent with population expansions associated with the warming climate after the LGM when the faster mutation rate is applied.

Ecological effects on population genetic patterns

We observed both mitochondrial and nuclear genetic evidence indicating that differences in the ecology of two closely related, codistributed species have an impact on population genetic structure. The two species show similar mtDNA divergence, suggesting that their length of occupancy within the southern stable region is comparable. The generalist ecology of *D. merriami*, however, leads to higher population densities (Brown 1973) which should lead to higher levels of genetic diversity within populations. We indeed recovered higher mtDNA diversity and estimated effective population sizes (N_e) in *D. merriami* compared to the substrate specialist *D. deserti* (Fig. 3, insets; Fig. 4A). Conversely, nuclear indices of diversity, including the percentage of polymorphic loci, nucleotide diversity and heterozygosity, were similar in the southern stable populations of both species (Fig. 5A–C). These nuclear indices remained comparable even when we analysed each stable locality separately (the two sampling sites were identical for both species, Fig. 1): 0.0044 and 0.0046 for *D. deserti* and 0.0048 and 0.0045 for *D. merriami* using the 10× coverage, 75% individuals across loci threshold. It is not clear precisely why *D. merriami* does not exhibit higher levels of nuclear diversity than *D. deserti*, although ecological characteristics not accounted for in this study (e.g. differential home ranges and male dispersal rates between the two species) may influence such patterns of nuclear diversity at a local scale.

Differentiation among stable and expanded populations represented by mitochondrial pairwise genetic distances (Fig. 4C) and nuclear F_{ST} values (Fig. 6) was expected to be higher in the substrate specialist *D. deserti* due to its more fragmented distribution, which may impact levels of gene flow, and both nuclear and mtDNA data support this prediction (Fig. 6). Private allele and haplotype frequencies were also expected to be higher in *D. deserti*, because species with a more fragmented distribution should exhibit limited gene exchange among populations (Collado & Mendez 2013). Our mtDNA data do not support this prediction, possibly because of limited sampling per sampling locality that prevented robust estimates of private haplotype frequencies within populations (Fig. 4B). Private allele frequencies were not significantly different between the two species although a nonsignificant trend of higher private allele frequency in the stable areas for *D. deserti* is consistent with our prediction (Fig. 5D).

Genetic consequences of range expansions with respect to ecology

We found evidence for the synergistic effect of historical population expansion and species-specific ecology on population genetic patterns. The rate at which the indices of genetic variation decrease along an axis of

population expansion is predicted to be exponentially proportional to the effective population size at the colonization front (Wegmann *et al.* 2006; Excoffier *et al.* 2009). Accordingly, in habitat specialists with greater natural population fragmentation, the number of migrants involved in a range expansion should be smaller, and genetic variation should decrease more rapidly in the direction of expansion (Excoffier *et al.* 2009; Banks *et al.* 2010; Smit *et al.* 2010).

Patterns of genetic variation observed based on mtDNA corresponded very well with these expectations. Mitochondrial nucleotide diversity, private haplotype frequencies and genetic differentiation (pairwise genetic distances) decrease more rapidly in the direction of the expansion in *D. deserti* compared with *D. merriami* (Fig. 4), with the latter species exhibiting comparable nucleotide diversities in stable and expanded areas (Fig. 4A). We believe that the lack of decreased mtDNA diversity in post-LGM expanded areas in *D. merriami* is likely linked to its larger effective population sizes, wider colonization front and possibly multiple northward colonization routes.

Given evidence from mtDNA that post-LGM expansion leads to more extreme loss of genetic diversity in the substrate specialist *D. deserti*, we asked whether nuclear genetic variation followed this pattern. We found that patterns of nuclear variation were qualitatively consistent with the mtDNA patterns of variation and our predictions. Like the mtDNA data, the frequency of nuclear private alleles decreased more rapidly in the northern populations of *D. deserti* than in *D. merriami* (Fig. 5D). Patterns of nuclear genetic diversity and heterozygosity also suggest greater loss in both measures in expanded populations of *D. deserti*, with little or no decrease in *D. merriami* (Fig. 5B,C). Importantly, the decrease in nuclear diversity in *D. deserti* was quantitatively much smaller, 200-fold smaller, than the decrease in mtDNA (we observed a 0.2-fold decrease in nuclear diversity but 10-fold decrease in mtDNA diversity; Fig. 5B). The smaller effective population sizes of mtDNA coupled with higher migration rates in males (documented in other *Dipodomys* species; Zeng & Brown 1987) may explain why mtDNA variation experienced greater decrease in expanded populations of *D. deserti* than did nuclear diversity (Figs 4A and 5B).

Quantitative discordance in mitochondrial vs. nuclear patterns of genetic variation

Our results suggest that ecological characteristics and historical population processes may play a more deterministic or pronounced role in generating patterns of mtDNA genetic variation, whereas nuclear genetic variation may be more robust to the effects of ecology and historical processes. Specifically, we found that patterns of decreased mtDNA diversity in response to different ecologies and postglacial geographic expansion are not necessarily accompanied by quantitatively comparable reductions in nuclear genomic diversity. We presume that this effect is the result of the smaller effective population sizes of mtDNA and/or sex-biased patterns of gene flow.

Our findings have two major implications. First, they suggest that mtDNA estimates may be more sensitive for the detection of past population expansion and geographic patterns of expansion. Second, they indicate that mtDNA-based estimates may be a poor predictor of nuclear genetic diversity in expanded populations and, accordingly, be a poor indicator of the extent to which expanded populations are susceptible to reduced fitness and reduced potential to evolve in response to climate change.

Acknowledgements

We thank A. Ambos, Akira, L. Alexander, Z. Marshall, B. Smith and J. Jaeger (JRJ) for help with sampling; J. Castoe, R. Adams, R. Wostl and R. Carson for help in the laboratory; J. Klicka for allowing us to use his laboratory to process skin samples; the New Mexico Museum of Natural History and P. Gegick for curatorial support; and the Museum of Vertebrate Zoology for loaning of tissue samples. This work was supported by faculty start-up funds from UTA to TAC, UNLV President's Research Award to BRR and JRJ, NSF EPSCoR Grants SFFA UCCSN 02-123 and EPS-0814372 to TJ and MEE, NSF Doctoral Dissertation Improvement Grant DEB-0808565 to TJ, American Society of Mammalogists Grants-In-Aid to TJ and MEE, and a Major Research Instrumentation Grant DBI-0421519 to the University of Nevada, Las Vegas.

References

Alexander LF, Riddle BR (2005) Phylogenetics of the new world rodent family heteromyidae. *Journal of Mammalogy*, **86**, 366–379.

Austerlitz F, Jung-Muller B, Godelle B, Gouyon PH (1997) Evolution of coalescence times, genetic diversity and structure during colonization. *Theoretical Population Biology*, **51**, 148–164.

Avolio ML, Beaulieu JM, Lo EYY, Smith MD (2012) Measuring genetic diversity in ecological studies. *Plant Ecology*, **213**, 1105–1115.

Bandelt HJ, Forster P, Rohl A (1999) Median-joining networks for inferring intraspecific phylogenies. *Molecular Biology and Evolution*, **16**, 37–48.

Banks SC, Ling SD, Johnson CR *et al.* (2010) Genetic structure of a recent climate change-driven range extension. *Molecular Ecology*, **19**, 2011–2024.

Best TL, Hildreth NJ, Jones C (1989) *Dipodomys deserti*. *Mammalian Species*, **339**, 1–8.

Bialozyt R, Ziegenhagen B, Petit RJ (2006) Contrasting effects of long distance seed dispersal on genetic diversity during range expansion. *Journal of Evolutionary Biology*, **19**, 12–20.

Boria RA, Olson LE, Goodman SM, Anderson RP (2014) Spatial filtering to reduce sampling bias can improve the performance of ecological niche models. *Ecological Modelling*, **275**, 73–77.

Braconnot P, Otto-Bliesner B, Harrison S *et al.* (2007) Results of PMIP2 coupled simulations of the Mid-Holocene and Last Glacial Maximum—Part 1: experiments and large-scale features. *Climate of the Past*, **3**, 261–277.

Britten HB, Rust RW (1996) Population structure of a sand dune-obligate beetle, *Eusattus muricatus*, and its implications for dune management. *Conservation Biology*, **10**, 647–652.

Brown JH (1973) Species diversity of seed eating desert rodents in sand dune habitats. *Ecology*, **54**, 775–787.

Catchen JM, Amores A, Hohenlohe P, Cresko W, Postlethwait JH (2011) Stacks: building and genotyping loci de novo from short-read sequences. *G3: Genes, Genomes, Genetics*, **1**, 171–182.

Chan YL, Lacey EA, Pearson OP, Hadly EA (2005) Ancient DNA reveals Holocene loss of genetic diversity in a South American rodent. *Biology Letters*, **1**, 423–426.

Collado GA, Mendez MA (2013) Microgeographic differentiation among closely related species of Biomphalaria (Gastropoda: Planorbidae) from the Andean Altiplano. *Zoological Journal of the Linnean Society*, **169**, 640–652.

Draheim HM, Baird P, Haig SM (2012) Temporal analysis of mtDNA variation reveals decreased genetic diversity in least terns. *Condor*, **114**, 145–154.

Drummond AJ, Rambaut A (2007) BEAST: Bayesian evolutionary analysis by sampling trees. *Bmc Evolutionary Biology*, **7**, 214.

Drummond AJ, Rambaut A, Shapiro B, Pybus OG (2005) Bayesian coalescent inference of past population dynamics from molecular sequences. *Molecular Biology and Evolution*, **22**, 1185–1192.

Elith J, Graham CH, Anderson RP *et al.* (2006) Novel methods improve prediction of species' distributions from occurrence data. *Ecography*, **29**, 129–151.

Elith J, Kearney M, Phillips S (2010) The art of modelling range-shifting species. *Methods in Ecology and Evolution*, **1**, 330–342.

Excoffier L, Laval G, Schneider S (2005) Arlequin (version 3.0): an integrated software package for population genetics data analysis. *Evolutionary Bioinformatics Online*, **1**, 47–50.

Excoffier L, Foll M, Petit RJ (2009) Genetic consequences of range expansions. *Annual Review of Ecology Evolution and Systematics*, **40**, 481–501.

Galbreath KE, Hafner DJ, Zamudio KR (2009) When cold is better: climate-driven elevation shifts yield complex patterns of diversification and demography in an alpine specialist (American pika, *Ochotona princeps*). *Evolution*, **63**, 2848–2863.

Graham MR, Jaeger JR, Prendini L, Riddle BR (2013) Phylogeography of Beck's Desert Scorpion, *Paruroctonus becki*, reveals Pliocene diversification in the Eastern California Shear Zone and postglacial expansion in the Great Basin Desert. *Molecular Phylogenetics and Evolution*, **69**, 502–513.

Grassi F, Minuto L, Casazza G, Labra M, Sala F (2009) Haplotype richness in refugial areas: phylogeographical structure of *Saxifraga callosa*. *Journal of Plant Research*, **122**, 377–387.

Grayson DK (1993) *The Desert's Past. A Natural Prehistory of the Great Basin*. Smithsonian Institute Press, Washington, District of Columbia.

Hallatschek O, Nelson DR (2008) Gene surfing in expanding populations. *Theoretical Population Biology*, **73**, 158–170.

Hewitt GM (1996) Some genetic consequences of ice ages, and their role in divergence and speciation. *Biological Journal of the Linnean Society*, **58**, 247–276.

Hewitt GM (2000) The genetic legacy of the Quaternary ice ages. *Nature*, **405**, 907–913.

Hijmans RJ, Cameron SE, Parra JL, Jones PG, Jarvis A (2005) Very high resolution interpolated climate surfaces for global land areas. *International Journal of Climatology*, **25**, 1965–1978.

Hill MP, Hoffmann AA, Macfadyen S, Umina PA, Elith J (2012) Understanding niche shifts: using current and historical data to model the invasive redlegged earth mite, *Halotydeus destructor*. *Diversity and Distributions*, **18**, 191–203.

Hockett BS (2000) Paleobiogeographic changes at the Pleistocene-Holocene boundary near Pintwater Cave, southern Nevada. *Quaternary Research*, **53**, 263–269.

Jezkova T (2010) *Reconstructing Species Responses to Past Climatic Changes Using Niche Modeling and Genetic Data*. University of Nevada, Las Vegas, Nevada.

Jezkova T, Olah-Hemmings V, Riddle BR (2011) Niche shifting in response to warming climate after the last glacial maximum: inference from genetic data and niche assessments in the chisel-toothed kangaroo rat (*Dipodomys microps*). *Global Change Biology*, **17**, 3486–3502.

Jones KB (1995) *Phylogeography of the Desert Horned Lizard (Phrynosoma platyrhinos) and the Short-Horned Lizard (Phrynosoma douglassii): Patterns of Divergence and Diversity*. University of Nevada, Las Vegas, Nevada.

Jones FC, Grabherr MG, Chan YF *et al.* (2012) The genomic basis of adaptive evolution in threespine sticklebacks. *Nature*, **484**, 55–61.

Joyce DA, Pullin AS (2003) Conservation implications of the distribution of genetic diversity at different scales: a case study using the marsh fritillary butterfly (*Euphydryas aurinia*). *Biological Conservation*, **114**, 453–461.

Kerdelhue C, Zane L, Simonato M *et al.* (2009) Quaternary history and contemporary patterns in a currently expanding species. *Bmc Evolutionary Biology*, **9**, 1–14.

Kocher TD, Thomas WK, Meyer A *et al.* (1989) Dynamics of mitochondrial DNA evolution in animals—amplification and sequencing with conserved primers. *Proceedings of the National Academy of Sciences of the United States of America*, **86**, 6196–6200.

Lacy RC (1997) Importance of genetic variation to the viability of mammalian populations. *Journal of Mammalogy*, **78**, 320–335.

Liu CR, Berry PM, Dawson TP, Pearson RG (2005) Selecting thresholds of occurrence in the prediction of species distributions. *Ecography*, **28**, 385–393.

Maggs CA, Castilho R, Foltz D *et al.* (2008) Evaluating signatures of glacial refugia for North Atlantic benthic marine taxa. *Ecology*, **89**, S108–S122.

Martin AP, Palumbi SR (1993) Body size, metabolic rate, generation time, and the molecular clock. *Proceedings of the National Academy of Sciences of the United States of America*, **90**, 4087–4091.

Mila B, Girman DJ, Kimura M, Smith TB (2000) Genetic evidence for the effect of a postglacial population expansion

on the phylogeography of a North American songbird. *Proceedings of the Royal Society B-Biological Sciences*, **267**, 1033–1040.

Miller MP (2005) Alleles In Space (AIS): computer software for the joint analysis of interindividual spatial and genetic information. *Journal of Heredity*, **96**, 722–724.

Mulcahy DG (2008) Phylogeography and species boundaries of the western North American Nightsnake (*Hypsiglena torquata*): revisiting the subspecies concept. *Molecular Phylogenetics and Evolution*, **46**, 1095–1115.

Ouborg NJ (2010) Integrating population genetics and conservation biology in the era of genomics. *Biology Letters*, **6**, 3–6.

Peterson BK, Weber JN, Kay EH, Fisher HS, Hoekstra HE (2012) Double digest RADseq: an inexpensive method for *de novo* SNP discovery and genotyping in model and non-model species. *PLoS ONE*, **7**, e37135.

Phillips SJ, Dudik M (2008) Modeling of species distributions with Maxent: new extensions and a comprehensive evaluation. *Ecography*, **31**, 161–175.

Phillips SJ, Dudik M, Schapire RE (2004) A maximum entropy approach to species distribution modeling. In: *Proceedings of the Twenty-First International Conference on Machine Learning*, pp. 655–662. ACM, New York, NY, USA, Banff, Alberta, Canada.

Phillips SJ, Anderson RP, Schapire RE (2006) Maximum entropy modeling of species geographic distributions. *Ecological Modelling*, **190**, 231–259.

R Development Core Team (2008) *R: A Language and Environment for Statistical Computing*. R Development Core Team, Vienna, Austria.

Radosavljevic A, Anderson RP (2014) Making better MAXENT models of species distributions: complexity, overfitting and evaluation. *Journal of Biogeography*, **41**, 629–643.

Raes N, ter Steege H (2007) A null-model for significance testing of presence-only species distribution models. *Ecography*, **30**, 727–736.

Reheis MC (1999) Extent of Pleistocene lakes in the western Great Basin. In: *US Geological Survey Miscellaneous Field Studies Map MF-2323*. US Geological Survey, Denver, Colorado.

Sikes RS, Gannon WL, Amer Soc M (2011) Guidelines of the American Society of Mammalogists for the use of wild mammals in research. *Journal of Mammalogy*, **92**, 235–253.

Smit HA, Watson J, van Vuuren BJ (2010) Relative importance of habitat connectivity in shaping the genetic profiles of two southern African elephant-shrews. *Journal of Biogeography*, **37**, 857–864.

Smith RS (1993) Sand dunes in the North American deserts. In: *Reference Handbook of the Deserts of North America* (ed. Bender GL), pp. 481–524. Greenwood Press, Westport, Connecticut.

Smith BT, Escalante P, Banos BEH *et al.* (2011) The role of historical and contemporary processes on phylogeographic structure and genetic diversity in the Northern Cardinal, *Cardinalis cardinalis*. *Bmc Evolutionary Biology*, **11**, 1–12.

Spaulding WG (1983) Late Wisconsin macrofossil records of desert vegetation in the American Southwest. *Quaternary Research*, **19**, 256–264.

Spaulding WG (1990a) Vegetation dynamics during the last deglaciation, southeastern Great Basin, USA. *Quaternary Research*, **33**, 188–203.

Spaulding WG (1990b) Vegetational and climatic development of the Mojave Desert: the last glacial maximum to the present. In: *In Packrat Middens: The Last 40,000 Years of Biotic Change* (eds Betancourt JL, Van Devender TR & Martin PS), pp. 166–199. The University of Arizona Press, Tucson, Arizona.

Spradling TA, Hafner MS, Demastes JW (2001) Differences in rate of cytochrome-*b* evolution among species of rodents. *Journal of Mammalogy*, **82**, 65–80.

Spradling TA, Tamplin JW, Dow SS, Meyer KJ (2010) Conservation genetics of a peripherally isolated population of the wood turtle (*Glyptemys insculpta*) in Iowa. *Conservation Genetics*, **11**, 1667–1677.

Stone JL, Crystal PA, Devlin EE, Downer RHL, Cameron DS (2012) Highest genetic diversity at the northern range limit of the rare orchid *Isotria medeoloides*. *Heredity*, **109**, 215–221.

Tamura K, Peterson D, Peterson N *et al.* (2011) MEGA5: molecular evolutionary genetics analysis using maximum likelihood, evolutionary distance, and maximum parsimony methods. *Molecular Biology and Evolution*, **28**, 2731–2739.

Thompson RS (1990) Late Quaternary vegetation and climate in the Great Basin. In: *Packrat Middens; The Last 40,000 Years of Biotic Change* (eds Betancourt JL, Van Devender TR, Martin PS), pp. 200–239. The University of Arizona Press, Tucson, Arizona.

Watson DF, Philip GM (1985) A refinement of inverse distance weighted interpolation. *Geo-Processing*, **2**, 315–327.

Wegmann D, Currat M, Excoffier L (2006) Molecular diversity after a range expansion in heterogeneous environments. *Genetics*, **174**, 2009–2020.

White TA, Perkins SE, Heckel G, Searle JB (2013) Adaptive evolution during an ongoing range expansion: the invasive bank vole (*Myodes glareolus*) in Ireland. *Molecular Ecology*, **22**, 2971–2985.

Young A, Boyle T, Brown T (1996) The population genetic consequences of habitat fragmentation for plants. *Trends in Ecology & Evolution*, **11**, 413–418.

Zeng ZY, Brown JH (1987) Population ecology of a desert rodent, *Dipodomys merriami*, in the Chihuahuan Desert. *Ecology*, **68**, 1328–1340.

T.J., B.R.R. and T.A.C. designed the research; T.J. collected the samples; T.J., D.C.C. and D.R.S. generated the genetic data; T.J., D.C.C., D.R.S., T.A.C. and M.E.E. analysed the data; T.J. and T.A.C. wrote the manuscript; B.R.R. and T.A.C. contributed reagents/materials; all authors critically revised and approved the final manuscript.

Data accessibility

DNA sequences: GenBank accession nos KP059295–KP059622 (mtDNA data, *Dipodomys deserti*), KP059623–KP059832 (mtDNA data, *Dipodomys merriami*), and

BioProject PRJNA266492 and Dryad doi: 10.5061/dryad.1nv6k (RADseq data). Sampling locations uploaded as online supplemental material (Data S1, Supporting information). DNA sequence alignments and read mapping: Dryad doi: 10.5061/dryad.1nv6k. Complete STACKS catalog: Dryad doi: 10.5061/dryad.1nv6k.

Supporting information

Additional supporting information may be found in the online version of this article.

Fig. S1 Climatic niche models built using sampling sites.

Fig. S2 Correlations of nucleotide diversity (A) and private haplotypes (B) with samples size for *Dipodomys deserti* (left column) and *Dipodomys merriami* (right column).

Data S1 Samples of *Dipodomys deserti* and *Dipodomys merriami* sorted by Country, State and County.

Table S1 Statistics based on the number of reads retained after processing steps in the ddRAD pipeline for each sample: number of quality filtered reads, the number of mapped reads, and the ultimate number of loci at 10× and 20× coverage.